

## Supplementary Information for

### **A two-fold engineering approach based on Bi<sub>2</sub>Te<sub>3</sub> flakes towards efficient and stable inverted perovskite solar cells**

Dimitris Tsikritzis,<sup>a</sup> Konstantinos Rogdakis<sup>a</sup>, Konstantinos Chatzimanolis,<sup>a</sup> Miloš Petrović,<sup>a</sup> Nikos Tzoganakis,<sup>a</sup> Leyla Najafi,<sup>b,c</sup> Beatriz Martín-García,<sup>b,d</sup> Reinier Oropesa-Nuñez,<sup>c,e</sup> Sebastiano Bellani,<sup>b,c</sup> Antonio Esaù Del Rio Castillo,<sup>b,c</sup> Mirko Prato,<sup>f</sup> Minas M. Stylianakis,<sup>a</sup> Francesco Bonaccorso<sup>b,c,\*</sup> and Emmanuel Kymakis<sup>a,\*</sup>

a. Department of Electrical & Computer Engineering, Hellenic Mediterranean University, Heraklion 71410 Crete, Greece. E-mail: [kymakis@hmu.gr](mailto:kymakis@hmu.gr)

b. Graphene Labs, Istituto Italiano di Tecnologia, Via Morego 30, 16163 Genova, Italy Email: [Francesco.Bonaccorso@iit.it](mailto:Francesco.Bonaccorso@iit.it)

c. BeDimensional Spa., Via Albisola 121, 16163 Genova, Italy.

d. CIC nanoGUNE, 20018 Donostia-San Sebastian, Basque Country, Spain.

e. Department of Material Science and Engineering, Uppsala University, Box 534, 75121 Uppsala, Sweden.

f. Materials Characterization Facility, Istituto Italiano di Tecnologia, via Morego 30, 16163 Genova, Italy.

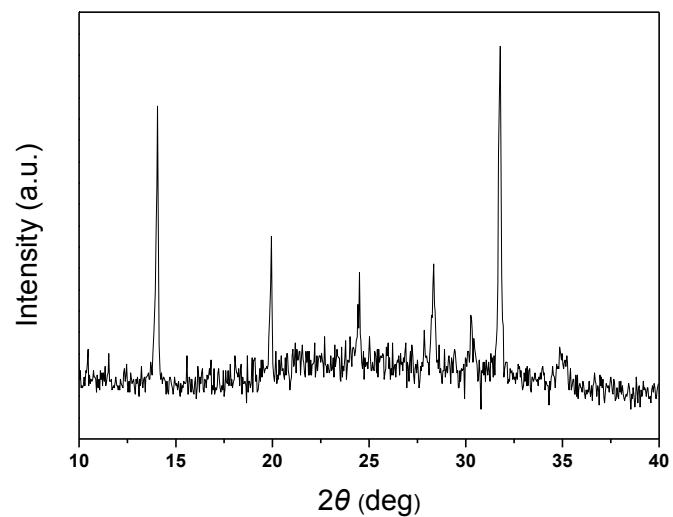


**Figure S1.** XRD pattern of the perovskite film

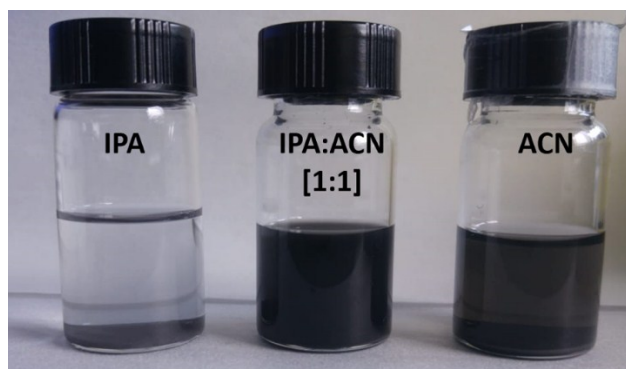


**Figure S2.** Photograph of the Bi<sub>2</sub>Te<sub>3</sub> flake dispersions produced by LPE in different solvent (IPA, ACN and IPA:ACN (1:1), after 4 h of gravitational sedimentation.

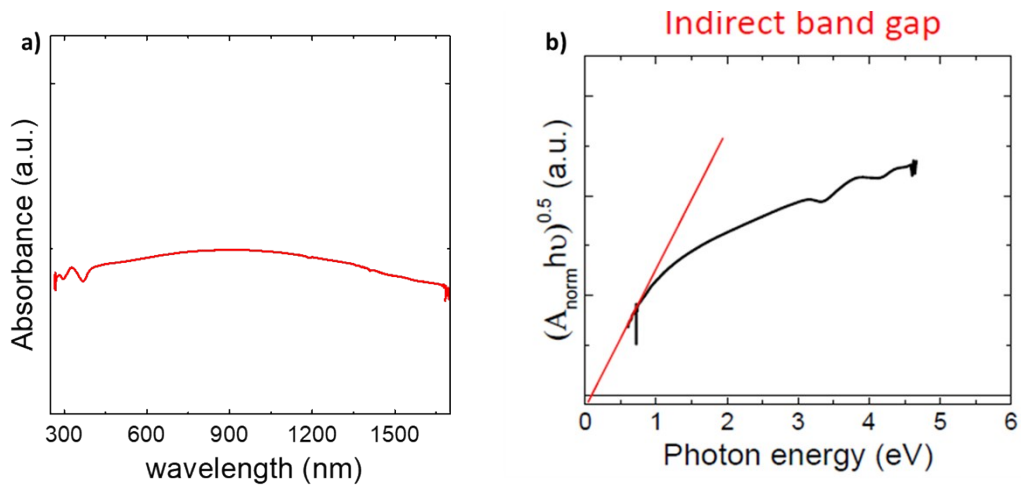


**Figure S3.** **a)** UV-Vis-NIR absorption measurement of the  $\text{Bi}_2\text{Te}_3$  flakes and **b)** Tauc plot analysis revealing the negligible band gap of the  $\text{Bi}_2\text{Te}_3$  flakes .

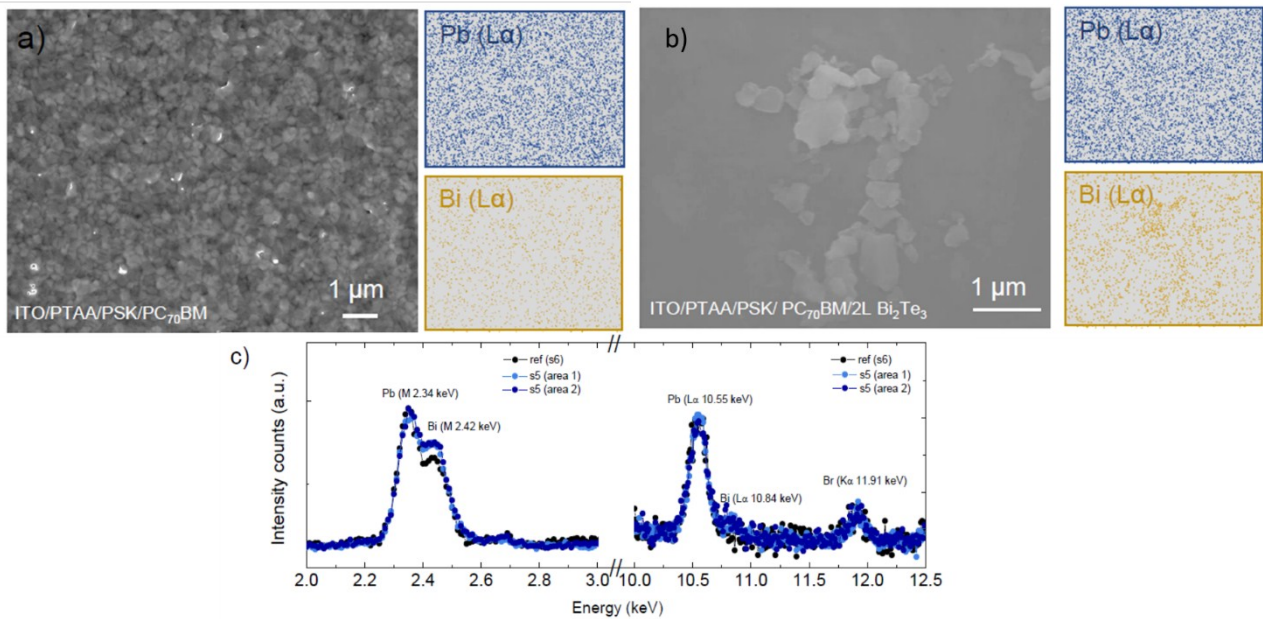


**Figure S4.** SEM images and EDX mapping of  $\text{PC}_{70}\text{BM}$  surface in **a)** PSC-Ref and **b)** PSC-Int2. The corresponding EDX maps for  $\text{Pb}$  ( $L\alpha = 10.55$  keV) and  $\text{Bi}$  ( $L\alpha = 11.84$  keV) are also shown. **(c)** Comparison of the EDX spectra collected for the reference (black) and two different areas for the PSC-Int2 (blue).

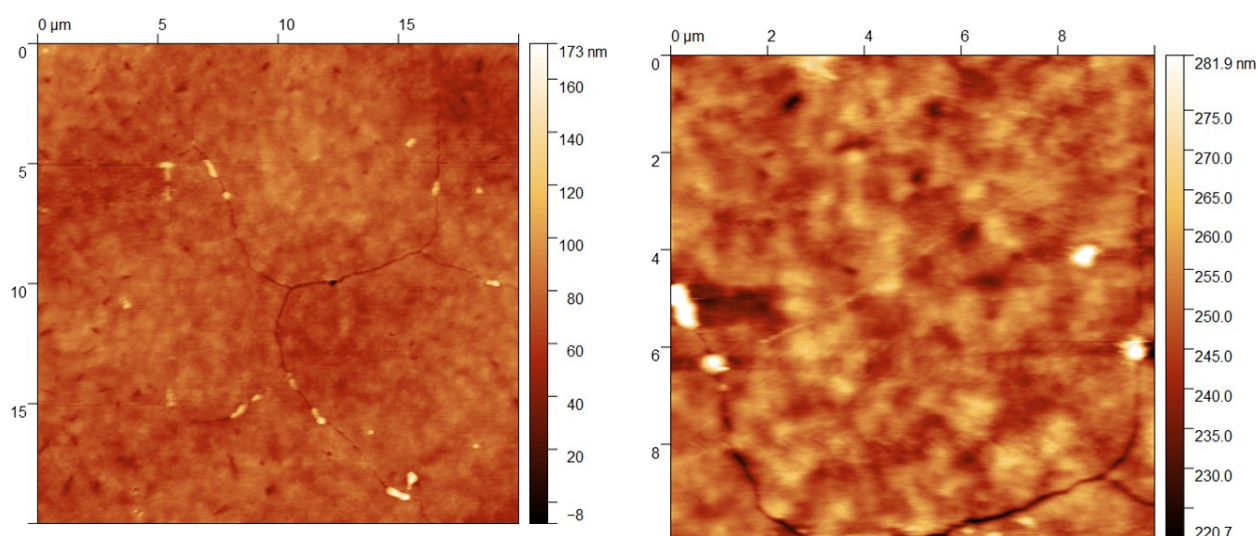


**Figure S5.** AFM images of the PC<sub>70</sub>BM surface with the Bi<sub>2</sub>Te<sub>3</sub> flakes spin coated (4SC) on top, noted as white spots. The left image spans an area of 20x20 μm<sup>2</sup> and the right a 10x10 μm<sup>2</sup>. Similarly, with SEM images, AFM images capture only the thick flakes due to resolution limitation.

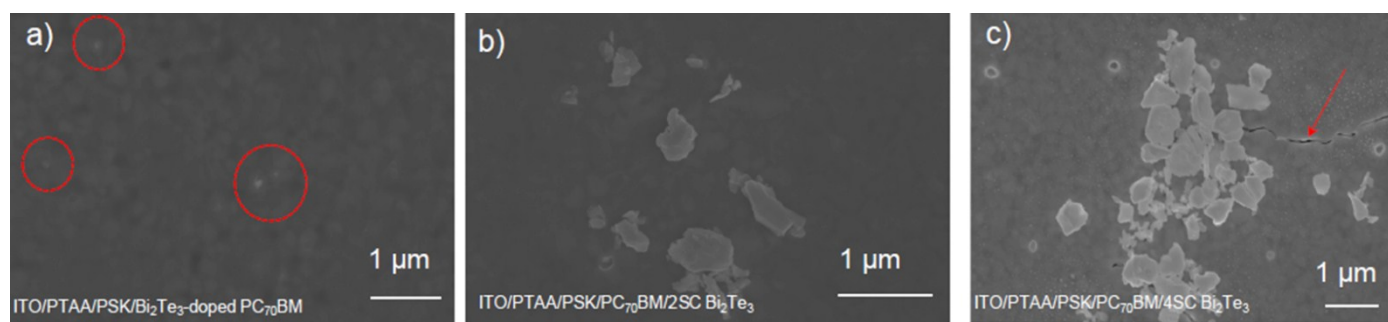


**Figure S6. a)** SEM image of PC<sub>70</sub>BM surface in PSC-Dop2 sample. The red circles show Bi<sub>2</sub>T<sub>3</sub> flakes in the PC<sub>70</sub>BM layer. Since we were using only the supernatant resulting from the solvent transfer of the Bi<sub>2</sub>T<sub>3</sub> flakes from IPA:ACN to chlorobenzene, only small and scattered flakes embedded into the ETL are visible in agreement with AFM images in Figure S3. **b-c)** SEM images revealing how by increasing the number of SC for the Bi<sub>2</sub>Te<sub>3</sub> interlayer formation promoted the formation of cracks (pointed out by an arrow) on ETL and/or perovskite layer, leading to low photovoltaic performance for SC>2 (see main text, Table 1).

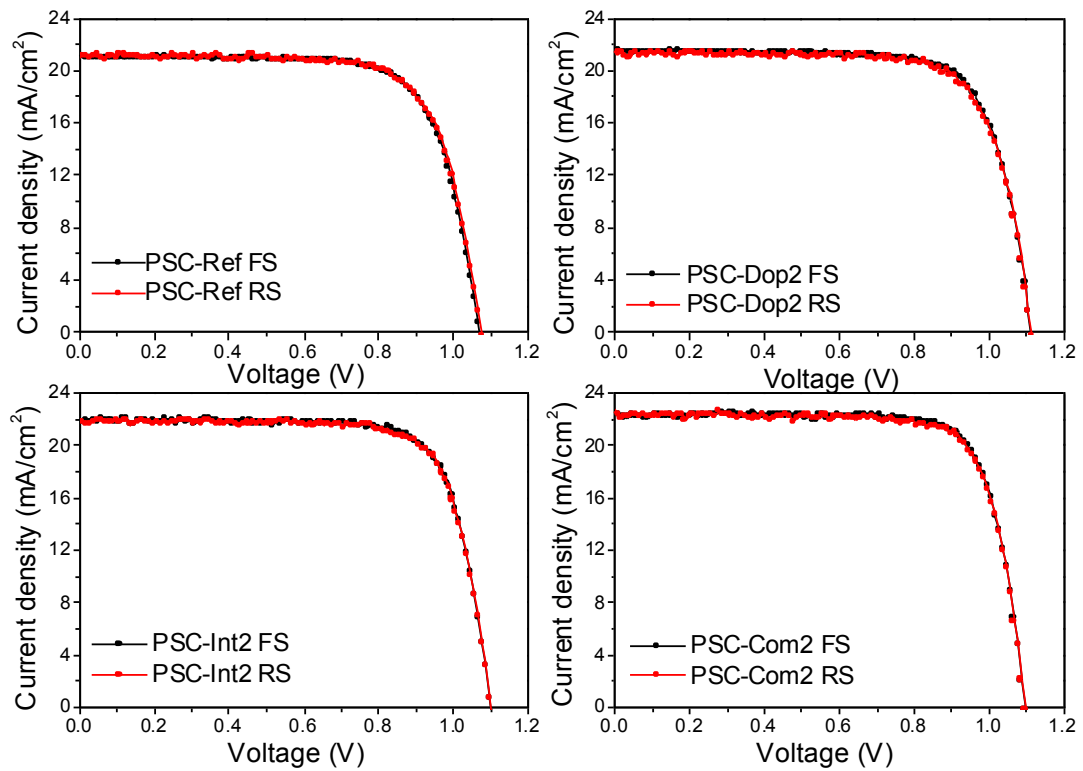


**Figure S7.** The forward (FS) and reverse (RS) scan J-V plots of the PSC devices

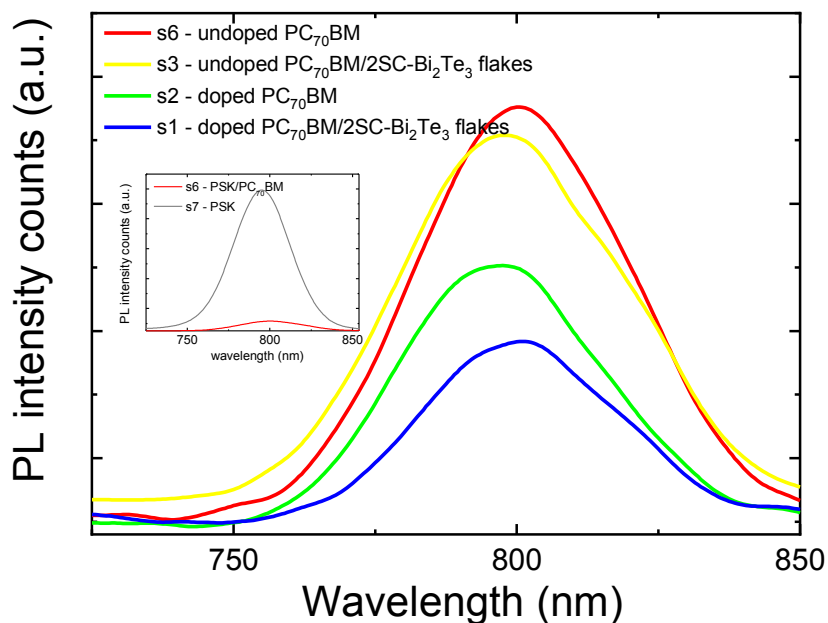


**Figure S8.** PL measurements of undoped PC<sub>70</sub>BM without (red) and with two spin coatings of Bi<sub>2</sub>Te<sub>3</sub> interlayer (yellow) on top. Besides, doped PC<sub>70</sub>BM without (green) and with 2 spin coatings of Bi<sub>2</sub>Te<sub>3</sub> interlayer (green) on top. In the inset: PL measurements of perovskite with and without PC<sub>70</sub>BM on top.

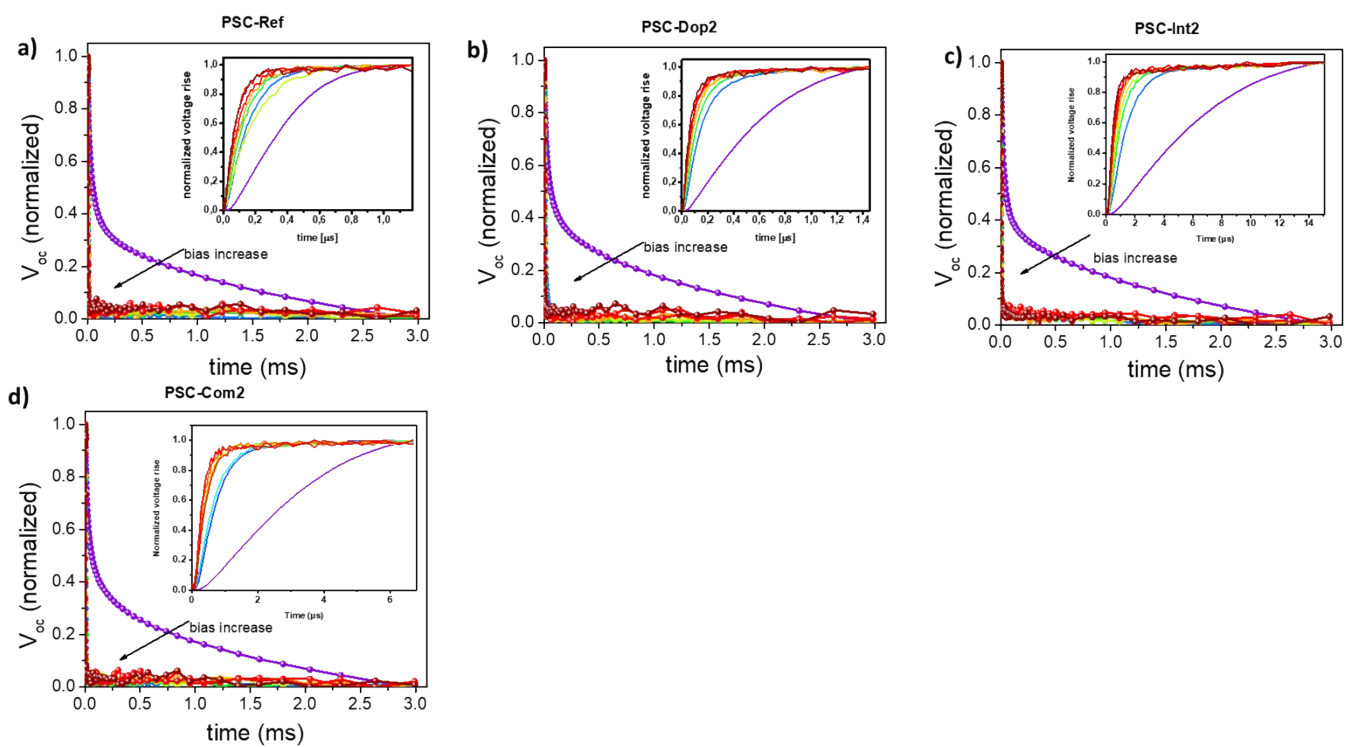


**Figure S9.** Raw data of TPV measurements of the devices: **a)** PSC-Ref, **b)** PSC-Dop2, **c)** PSC-Int2 and **d)** PSC-Com2. The insets present the voltage rise data.

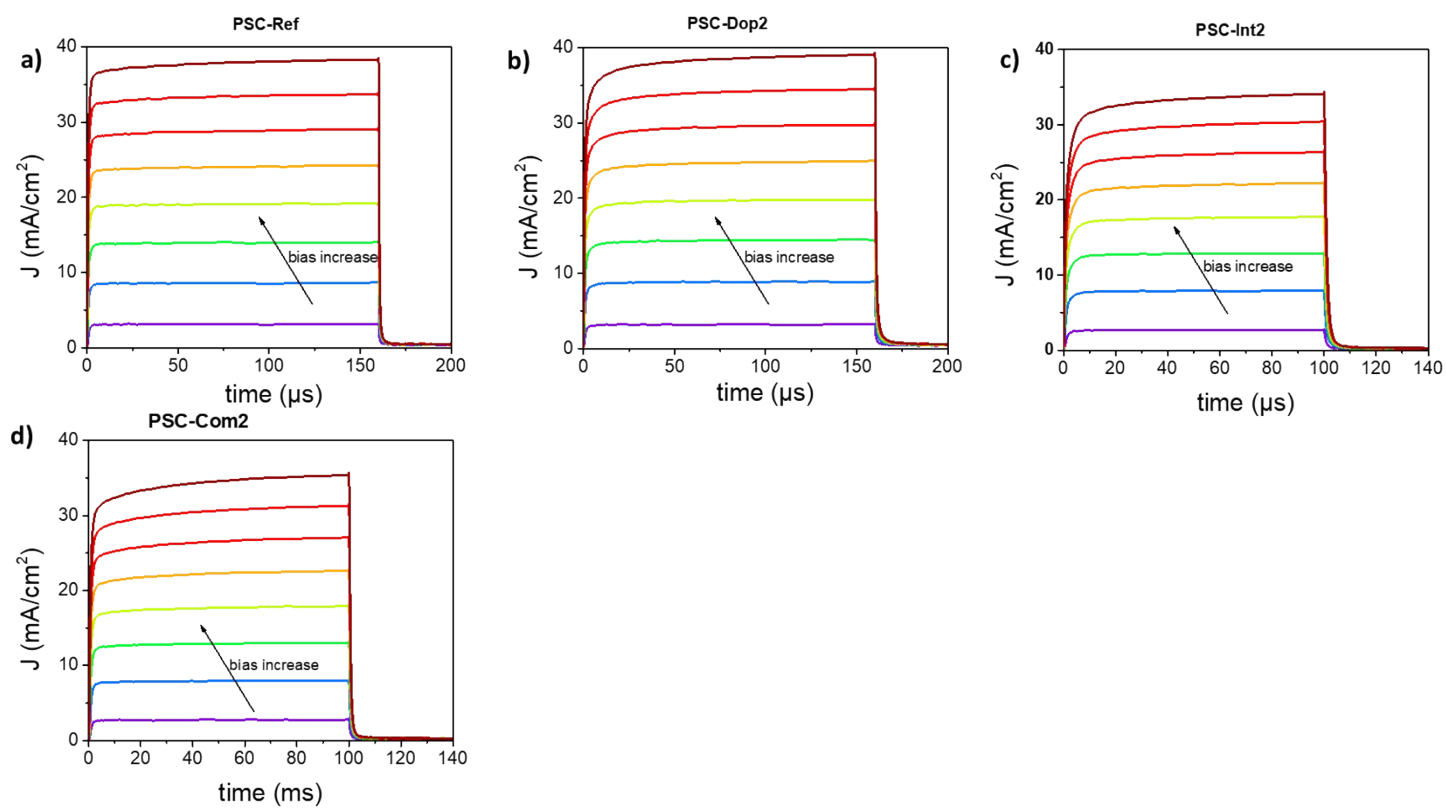


**Figure S10.** Raw data of various devices TPC measurements: **a)** PSC-Ref, **b)** PSC-Dop2, **c)** PSC-Int2 and **d)** PSC-Com2.

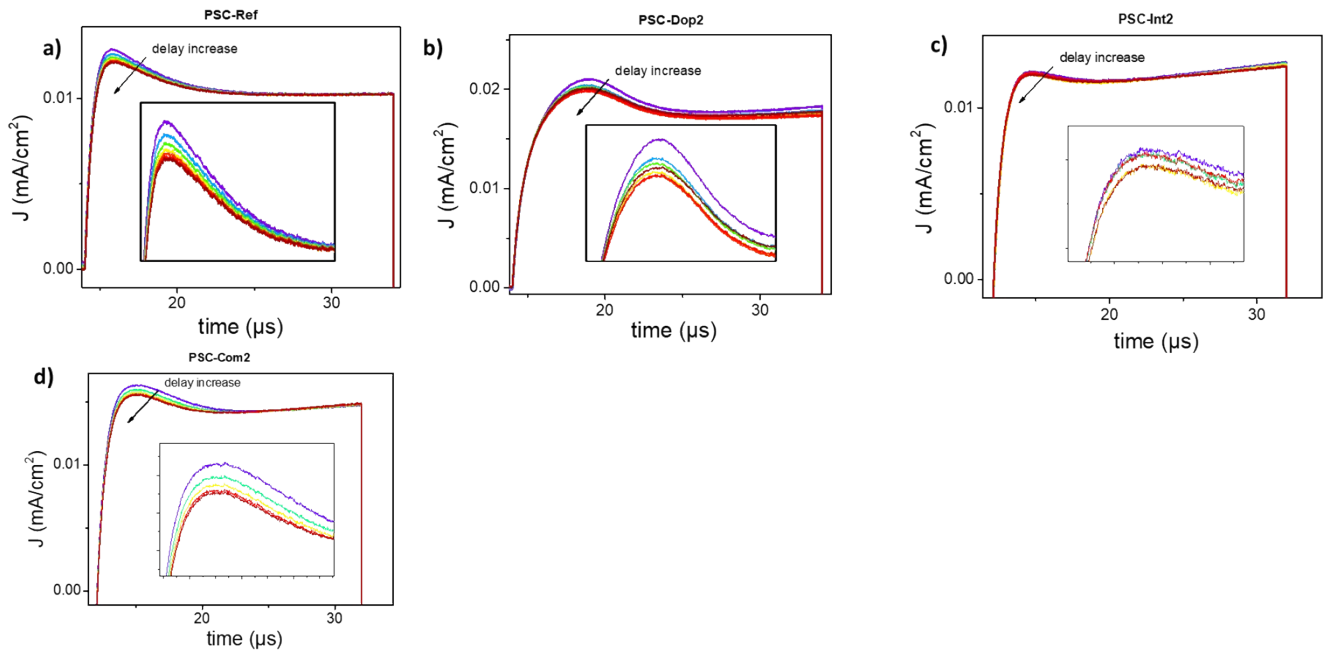


**Figure S11.** Raw data of photo-CELIV measurements used for the drift mobility extraction of the devices: **a)** PSC-Ref, **b)** PSC-Dop2, **c)** PSC-Int2 and **d)** PSC-Com2. The region near the peak is plotted in the insets.